RESEARCH PAPER | Physics | Volume : 3 | Issue : 5 | May 2013 | ISSN - 2249-555X

Structural and Optical Properties of Sm^{3+} ions in potassium niobate silicate glasses

KEYWORDS: silicate glasses; radiative properties; Judd- Ofelt theory; decay times

M. Murali Mohan	L. Rama Moorthy	C.K. Jayasankar
Department of Physics, Sri Venkateswara University, Tirupati-517 502, India	Department of Physics, Chadalavada Ramanamma Engineering College, Renugunta Road, Tirupati-517 506, India.	Department of Physics, Sri Venkateswara University, Tirupati-517 502, India

ABSTRACT

The trivalent samarium (Sm^{3+}) ions doped with potassium niobate silicate glasses (KNbSiSm) of molar composition 30 K_2O- 25 Nb_2O_5- (44.95- x) SiO2- xSm_2O_3 (where x= 0.05, 0.1, 0.5, 1.0 and 2.0 mol %) were prepared by conventional melt quenching technique. Raman spectrum was recorded to find out the basic structural units present in the title glass. Optical properties were characterized by using various spectroscopic techniques such as absorption, excitation, emission and decay measurements. The Judd- Ofelt intensity parameters (Ω_2, Ω_4 and Ω_6) have been derived from absorption spectrum which is in turn used to calculate radiative properties of the excited luminescent levels of Sm^{3+}- ions. The decay times of the $^4G_{5/2}$ excited level for different concentration of Sm^{3+}- ions have been measured. The non- exponential behavior of decay curves has been analyzed through Inokuti-Hirayama model. The characteristic emission and the radiative parameters obtained for the $^4G_{5/2} \rightarrow {}^6H_{7/2}$ transition indicate that the KNbSiSm glass could be very much useful for the development of lasers and photonic device applications in the visible region.

Summary: Potassium niobate silicate glasses with different concentrations of Sm^{3+}- ions were prepared and characterized for their structural and optical properties through Raman, absorption, excitation, emission and decay measurements at room temperature. The Raman spectrum revealed the basic structural units related to the presence of Si- O- Si and Nb- O bands which are attributed to NbO_6 octahedral with non-bridging oxygen's. Judd- Ofelt(JO) parameters Ω_λ (λ=2, 4, 6) have been evaluated from the oscillator strengths of absorption bands in UV- Vis/NIR regions. Various radiative parameters like radiative transition probabilities(A_R, s^{-1}), peak stimulated emission cross- sections $\sigma_e(\lambda_p)$, experimental (β_{exp}) and calculated (β_R) branching ratios for the emission transitions of Sm^{3+} ion in KNbSiSm10 glass. From these results it is suggested that Sm^{3+}-doped potassium niobate silicate glasses are more efficient luminescent materials for the development of lasers and photonic devices in the visible region.

1. Introduction

In recent years, rare earth doped glasses are found to be more useful materials for fiber amplifiers, sensors, high optical data storage/reading and solid state lasers [1, 2]. This is because of the fact, that the f-f electrons are shield by the outer 5s and 5p electrons, which lead to sharp absorption and emission lines due to weak interaction with the environment. Glass is a very important host material for the doping of rare earth ions for the development of optical devices. Among different types of glass systems, the oxide glasses are more suitable for practical applications due to their high chemical durability and thermal stability. In oxide glass, silicate glasses are the most popular hosts and easy to draw into fibers for use in lasers and fiber amplifiers [3]. Silicate glasses possess high transparency from near UV to IR spectral range, and high melting point, but the maximum phonon energy (~1100 cm^{-1}) is a still major problem due to the stretching vibrations of the network forming oxides. In these glasses, K_2O is often used to modify the field strength of cations to improve mechanical properties which is prerequisite for a good laser glass [4]. Moreover, glasses containing Nb_2O_5 exhibit good non-liner optical properties, such as high non-liner refractive index (n_2), which make them attractive materials for ultrafast switching devices [5]. Among rare earth ions, the Sm^{3+}- ions containing glass have stimulated extensive interest due their potential applications for high density optical storage, under sea communication and color displays [6]. In order to obtain optimum emission characteristics for device applications, the characteristic features of host material as well as the concentration dependent studies of Sm^{3+}- ions are very much essential. In this direction an extensive research has been carried out to identify the new glasses doped with Sm^{3+}- ions.

In the present study, the optical and structural properties of Sm^{3+}- ions in potassium niobate silicate glasses are investigated through the Raman, optical absorption, emission and decay curve analysis. The Judd-Ofelt[7, 8] intensity parameters (Ω_λ= 2, 4, 6) are determined from the measured oscillator strength of absorption bands of the KNbSiSm10 glass. Various radiative parameters have been evaluated and compared with those of the earlier reported systems [6, 17, 20].

2. Experimental details

2.1. Materials and methods

Sm^{3+}- doped potassium niobate silicate glasses (KNbSiSm) with a chemical composition of 30 K_2O- 25 Nb_2O_5- (44.95- x) SiO_2- xSm_2O_3, where x = 0.05, 0.1, 0.5, 1.0 and 2.0 mol %, were prepared by conventional melt quenching technique[6] and referred as KNbSiSm005, KNbSiSm01, KNbSiSm05, KNbSiSm10 and KNbSiSm20 respectively. The compositions of the batch materials (~15 g) were melted in a platinum crucible at 1350°C for about 2- 3 h. The melts were then poured onto a preheated brass mould at a temperature of 450°C and then the glass samples were annealed for 12 h to remove the thermal stress and strains and polished carefully for spectral measurements.

2.2. Physical and spectroscopic measurements

For 1.0 mol % Sm^{3+}- doped KNbSiSm10 glass, the physical parameters such as density (d = 3.37 g cm^{-3}), concentration(C = 1.47X10^{20} ions/cm^{-3}), optical path length (l = 0.396 cm) and the refractive index (n = 1.81) were determined. The Raman spectrum of the undoped sample was measured by Renishaw invia Raman microscope using 785 nm diode laser. The optical absorption spectrum of KNbSiSm10 glass was recorded using a Perkin Elmer Lambda-950 UV- Vis- NIR spectrophotometer in the wavelength range of 350- 2200 nm. The excitation and photoluminescence spectra were obtained by

Volume : 3 | Issue : 5 | May 2013 | ISSN - 2249-555X

exciting the samples at 404 nm and the decay measurements were done using Jobin Yvon Fluorolog-3 spectrofluorimeter using xenon arc lamp as an excitation source.

3. Results and discussion

3.1. Analysis of Raman spectrum

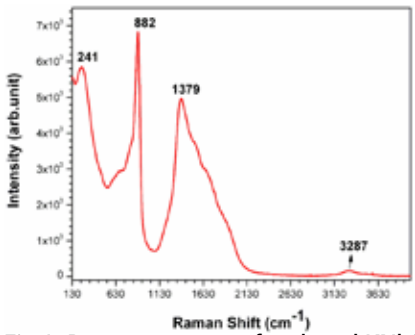

Fig.1. Raman spectrum of undoped KNbSi glass with 785 nm laser excitation

Structural details of the undoped KNbSi glass have been studied using Raman spectroscopy. The unpolarized Raman scattering spectrum measured using the 785 nm laser excitation exhibits four bands at 241, 882, 1379 and 3281 cm^{-1} as shown in Fig.1. It is noticed from Fig.1 that the high intensity phonon band at 882 cm^{-1} posses lesser energy than that of pure SiO_2 glass, which has a maximum phonon band around 1100 cm^{-1}[9]. The stretching modes of the Si-O-Si bands of SiO_4 tetrahedral with non-bridging oxygen atoms occur are active in the region 800-1300 cm^{-1} [10, 11] and the stretching modes of the Nb-O bonds in the NbO_6 octahedral occur in the 300-900 cm^{-1} region [12-14]. Particularly, the bands of SiO_4 occur at 1200, 1100, 950, 900, 850 cm^{-1}, while for the Nb-O in octahedral symmetry occurs at 870, 730, 625, and 340 cm^{-1}. The structural role of Nb_2O_5 in silicate, borate, germanate and gallate glasses has been investigated and found that NbO_6 groups exist in the glass network [15, 16]. Fukumi et.al[14] investigated the structural position of NbO_6- groups in K_2O- Nb_2O_5- SiO_2 glass systems and noticed the Raman band in the 800- 900 cm^{-1} region, which is attributed to NbO_6 octahedral with non-bridging oxygen and with much distortion. The broad bands in the 600- 800 cm^{-1} region are attributed to less distorted NbO_6 octahedral without non- bridging oxygen's. The bands at 815- 870 cm^{-1} are related to the Nb-O stretching modes of distorted NbO_6 octahedral sharing a corner with SiO_4 tetrahedral. As the Nb content increases, the NbO_6 octahedral as well as cluster start to appear, while the tetrahedral disappear. The characteristic intense band at 882 cm^{-1} is attributed to the presence of Si- O- Si and the band at 241 cm^{-1} is assigned to the presence of Nb- O. The characteristic bands around 1379 cm^{-1} and 3281 cm^{-1} are assigned to H- O- H vibration mode.

3.2. Absorption spectrum and Judd-Ofelt parameters

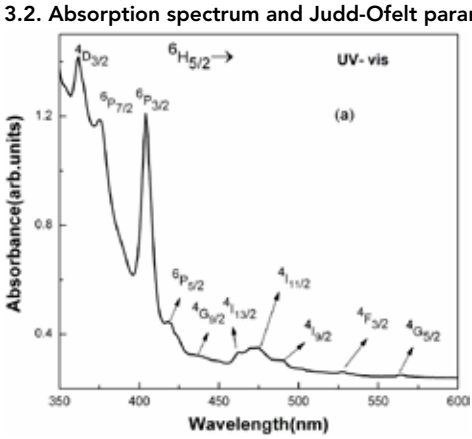

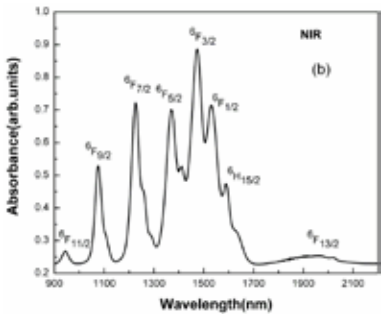

Fig.2. Optical absorption spectra of KNbSiSm10 glass (a) UV-Vis (b) NIR regions.

Optical absorption spectra of Sm^{3+}-doped KNbSiSm10 glass recorded in the ultraviolet (UV) - visible (Vis) and near infrared (NIR) regions are shown in Fig. 2(a) and 2(b) respectively. The shape and peak positions of Sm^{3+}- doped glasses [6, 17]. The spectra revealed sixteen absorption bands corresponding to the transition from the 6H5/2 ground state to the higher energy levels $^6H_{13/2}$, $^6H_{15/2}$, $^6F_{1/2}$, $^6F_{3/2}$, $^6F_{5/2}$, $^6F_{7/2}$, $^6F_{9/2}$, $^6F_{11/2}$, $^4G_{5/2}$, $^4F_{3/2}$, $4I_{13/2}$ + $^4I_{11/2}$ + $^4I_{9/2}$, $^4G_{9/2}$, $^6P_{5/2}$, $^6P_{3/2}$, $^6P_{7/2}$ and $^4D_{3/2}$. The assignment of absorption levels is done by comparing with energy levels of Sm^{3+}: aquo-ion [18]. The experimental oscillator strengths (ϕ_{exp}) of absorption bands determined from absorption spectrum are used to evaluate the JO parameters, $\Omega_\lambda(\lambda=2, 4, 6)$ by the least-square fit, which gives the best fit between the experimental (ϕ_{exp}) and calculated oscillator strength (ϕ_{cal}) as listed in Table 1.

Table1. Assignment of absorption transitions, energies (cm^{-1}), experimental (ϕ_{exp})and calculated (ϕ_{cal}) oscillator strengths (x 10^{-6}) for the absorption bands of Sm^{3+}- ion in KNbSiSm10 glass.

Transition $^6H_{5/2}\rightarrow$	Energy (cm^{-1})	KNbSiSm10	
		ϕ_{cal}	ϕ_{exp}
$^6H_{13/2}$	5178	0.46	0.63
$^6H_{15/2}$	6518	0.36	0.71
$^6F_{1/2}$	6277	0.78	0.60
$^6F_{3/2}$	6788	2.22	2.54
$^6F_{5/2}$	7304	3.71	3.45
$^6F_{7/2}$	8156	6.58	6.79
$^6F_{9/2}$	9293	4.46	4.34
$^6F_{11/2}$	10593	0.72	0.88
$^4G_{5/2}$	17730	0.24	0.04
$^4F_{3/2}$	18939	0.04	0.09
$^4I_{11/2}$	21097	1.42	2.12
$^4G_{9/2}$	22727	0.12	0.28
$^6P_{5/2}$	23809	1.08	0.85
$^6P_{3/2}$	24752	7.16	7.17
$^6P_{7/2}$	26595	2.67	1.18
$^4D_{3/2}$	27624	1.19	2.20
$\delta = \pm 0.54 \times 10^{-6}$			

The magnitudes of JO parameters (Ω_λ) are important for

Volume : 3 | Issue : 5 | May 2013 | ISSN - 2249-555X

the investigation of glass structure and the excited state dynamics of lanthanide (Ln^{3+}) ions. Generally, the Ω_2 parameter is sensitive to the symmetry of the rare earth ion site and strongly affected by covalence between rare earth ions and ligand anions, where as Ω_4 and Ω_6 are related to the rigidity of the host medium in which the ions are situated [19]. The magnitudes of Ω_2, Ω_4 and Ω_6, their trends and radiative lifetimes (τ_R, ms) for KNbSiSm10 glass are tabulated in Table. 2 along with the other reported systems [19- 20]. In the present investigation the trend of JO parameters have been observed as $\Omega_4 > \Omega_6 > \Omega_2$. Similar observation has been found for L5FBS10[19], tellurite[20], $Pb(PO_3)_2$[21], LBTAF [22], PbO-PbF_2[23], BLNS[24] and Calibo [25] glasses. Using these JO parameters, several radiative properties have been calculated as given in Table 3.

Table 2. Comparison of JO parameters (Ω_t, x10^{-20} cm^2), their trend and radiative lifetimes (τ_R, ms) of $^4G_{5/2}$ excited level in different Sm^{3+}- doped glasses.

Glass	Ω_2	Ω_4	Ω_6	Trend	τ_R	Reference
KNbSiSm 10	2.08	5.56	4.22	$\Omega_4 > \Omega_6 > \Omega_2$	1.6	Present work
L5FBS10	2.34	7.54	5.40	$\Omega_4 > \Omega_6 > \Omega_2$	2.15	[19]
Tellurite	0.06	0.34	0.24	$\Omega_4 > \Omega_6 > \Omega_2$	0.21	[20]
$Pb(PO_3)_2$	1.70	4.00	2.20	$\Omega_4 > \Omega_6 > \Omega_2$	2.75	[21]
LBTAF	0.27	2.52	2.47	$\Omega_4 > \Omega_6 > \Omega_2$	4.88	[22]
PbO-PbF_2	1.16	2.60	1.40	$\Omega_4 > \Omega_6 > \Omega_2$	4.46	[23]
BLNS	3.92	8.17	5.82	$\Omega_4 > \Omega_6 > \Omega_2$	2.88	[24]
Calibo	0.98	5.04	4.73	$\Omega_4 > \Omega_6 > \Omega_2$	3.97	[25]

Table3. Comparison emission peak positions (λ_p, nm), effective linewidths ($\Delta\lambda_{eff}$, nm), radiative transition probabilities (A, s^{-1}), peak stimulated emission cross-sections($\sigma(\lambda_p)$, x10^{-22} cm^2) calculated branching ratios (β_R) and experimental (β_{Exp}) for KNbSiSm10 glass with different Sm^{3+}-doped systems [6,17,20]

Transition	Parameters	KNbSiSm10 (present work)	Fluorophosphate [6]	Phosphate [17]	Tellurite [20]
$^4G_{5/2} \rightarrow H_{5/2}$					
	λ_p	567	562	563	563
	$\Delta\lambda_{eff}$	15.60	10.5	10.4	3.64
	A	37	24	28	2
	$\sigma(\lambda_p)$	1.10	1.27	1.21	5.50
	β_R	0.066	0.06	0.09	--
	$\beta_{(Exp.)}$	0.236	0.07	0.16	0.02
$^4G_{5/2} \rightarrow H_{7/2}$					
	λ_p	604	598	598	598
	$\Delta\lambda_{eff}$	15.86	12.3	10.4	6.04
	A	285	159	123	44
	$\sigma(\lambda_p)$	9.7	9.10	6.76	6.76
	β_R	0.505	0.41	0.40	---
	$\beta_{(Exp.)}$	0.457	0.39	0.52	0.49
$^4G_{5/2} \rightarrow {}^6H_{9/2}$					
	λ_p	651	645	645	643
	$\Delta\lambda_{eff}$	16.41	14.8	13.9	16.92
	A	171	124	126	19
	$\sigma(\lambda_p)$	7.574	8.01	7.06	2.57
	β_R	0.302	0.32	0.41	--
	$\beta_{(Exp.)}$	0.317	0.42	0.30	0.22
$^4G_{5/2} \rightarrow H_{11/2}$					
	λ_p	709	706	793	702
	$\Delta\lambda_{eff}$	28.23	21.5	41.9	5.44
	A	71	41	29	12
	$\sigma(\lambda_p)$	2.58	2.64	1.23	4.23
	β_R	0.13	0.11	0.10	---
	$\beta_{(Exp.)}$	0.02	0.12	0.02	0.13

3.3. Excitation spectrum

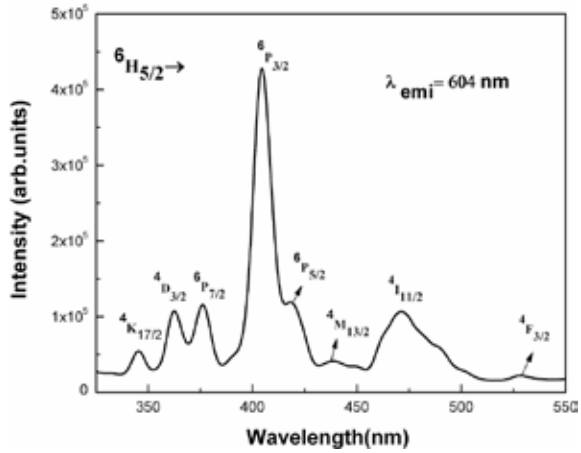

Fig.3. Excitation spectrum of KNbSiSm10 glass by monitoring the emission at 604 nm.

Fig. 3 shows the excitation spectrum of KNbSiSm10 glass by monitoring emission at 604 nm. Excitation spectrum is generally helpful to locate and assign more levels at higher energy side and also confirms the assignment of transitions made from absorption spectrum. In the 350- 550 nm region, the excitation bands identified are assigned to different electronic energy levels of $^4K_{17/2}$, $^4D_{3/2}$, $^6P_{7/2}$, $^6P_{3/2}$, $^6P_{5/2}$, $^4M_{13/2}$, $^4I_{11/2}$, and $^4F_{3/2}$ [26]. The excitation wavelength of 404 nm corresponding to the transition $^6H_{5/2} \rightarrow {}^6P_{3/2}$ has been used for the measurement of emission spectra of different concentration of Sm^{3+} ion doped glasses.

3.4. Emission spectra

The emission spectra for different concentrations of Sm^{3+}-doped KNbSiSm glasses under 404 nm excitation are shown in Fig. 4. The observed four emission peaks at 567, 604, 651 and 709 nm are assigned to $^4G_{5/2} \rightarrow {}^6H_{5/2}$, $^6H_{7/2}$, $^6H_{9/2}$ and $^6H_{11/2}$ transitions respectively [27]. These transitions are useful in high density optical storage, color displays and medical diagnostics. Among these the emission bands, the $^4G_{5/2} \rightarrow {}^6H_{7/2}$ transition at 604 nm posses highest intensity which leads to a bright reddish orange emission. Also the intensities of all the peaks increase with the increase of Sm^{3+}- ion concentration and reaches maximum at 0.5 mol % and beyond that the quenching has been observed. From luminescence spectra the peak wavelengths (λ_p, nm), effective bandwidths ($\Delta\lambda_{eff}$, nm), radiative transition probabilities (A_R, s^{-1}), peak stimulated emission cross-sections $\sigma_e(\lambda_p)$, branching ratios (β_R) and experimental branching ratios (β_{exp}) have been determined as listed in Table 3.

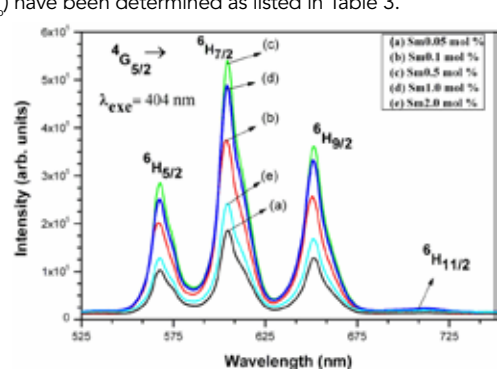

Fig.4. Photoluminescence spectra for different concentration of Sm3+ ions in KNbSiSm glasses under 404 nm excitation.

Volume : 3 | Issue : 5 | May 2013 | ISSN - 2249-555X

These evaluated radiative parameters are compared with those of Sm^{3+}- doped fluorophosphates [6], phosphate [17] and tellurite [20] glasses. It is observed that the transition probabilities (A_R, s^{-1}) and peak stimulated emission cross-sections $\sigma_e(\lambda_p)$ are high for all the emission transitions in the (KNbSiSm) glass. These results indicate that the $^4G_{5/2} \rightarrow {}^6H_{7/2}$ transition in KNbSiSm glass could be very much useful for the development of lasers and photonic devices in the visible region.

3.5. Decay curve analysis

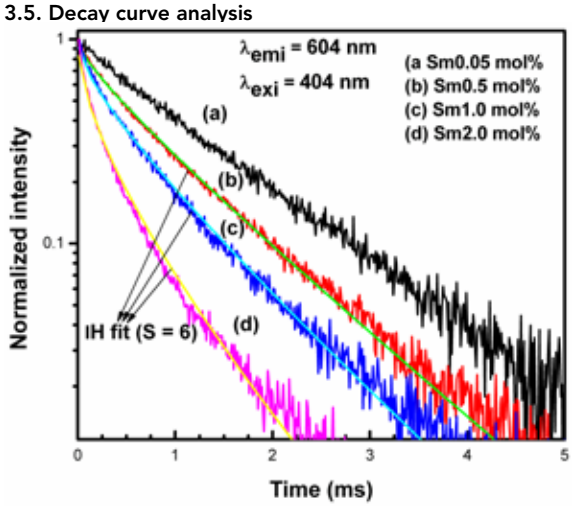

Fig.5. Decay curves for the $^4G_{5/2}$ level in for different concentrations of Sm^{3+}- ions in KNbSiSm glasses.

Fig. 5 shows the decay curves of $^4G_{5/2}$ excited level for different concentrations of Sm^{3+}- doped KNbSiSm glasses. The measured decay times are 1.19, 1.22, 0.93, 0.71 and 0.42 ms, for 0.05, 0.1, 0.5, 1.0, 2.0 mol % concentrations of Sm^{3+} ions, respectively. The decay curves at lower Sm^{3+} ion concentrations (≤ 0.1 mol %) exhibited single exponential nature, whereas at higher concentrations (≥ 0.5 mol %), the decay curves turned into non-exponential nature. The experimental lifetimes (τ_{exp}) of the $^4G_{5/2}$ level determined for KNbSiSm glasses are given in Table 4. The τ_{exp} values are found to decrease from 1.22 to 0.42 ms, when the concentration is increased from 0.1 to 2.0 mol % of Sm_2O_3. The decrease of τ_{exp} values indicates the presence of non-radiative energy transfer from the excited Sm^{3+}- ions to the neighboring unexcited Sm^{3+} ions. The non exponential decay curves are fitted to IH model [28] for S =6 as shown in Fig.5. The experimental lifetimes (τ_{exp}) along with the energy transfer parameters (Q), the donor-acceptor interaction parameters (C_{DA}) and critical transfer distances (R_0) have been calculated from the IH model as presented in Table.4. The analysis of non-exponential decay curves yields the values of energy transfer parameter 'Q', which increases from 0.54 to 2.02, with the increase of Sm^{3+} ions concentration from 0.5 to 2.0 mol %. The opposite trend has been observed in the case of critical transfer distances (R_0) and the donor-acceptor interaction parameters (C_{DA}). The magnitudes of 'Q' and 'C_{DA}' strongly depend on active ion and the glass composition. The non- exponentiality in the decay curves of rare earth doped materials usually arises due to the ion- ion interactions due to the increase of active ions concetration. The non- exponential nature of the decay curves with the increase of Sm^{3+}- ions concentration has been attributed to the energy transfer through cross-relaxation channels. The multiphonon relaxation rate in the case of Sm^{3+}- ions is negligible, since the energy gap between $^4G_{5/2}$ and next lower level $^6F_{11/2}$ is very large as can from the Fig. 6. The cross- relaxation channels that are responsible for the decrease τ_{exp} values of Sm^{3+}- ions are ($^4G_{5/2}$, $^6H_{5/2}$) → ($^6F_{5/2}$, $^6F_{11/2}$) and ($^4G_{5/2}$, $^6H_{5/2}$) → ($^6F_{9/2}$, $^6F_{7/2}$). Similar observations have been noticed for Sm^{3+}-ion in certain other reported glasses [6, 17].

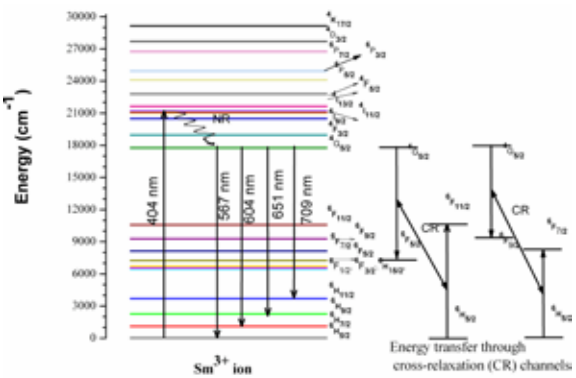

Fig.6. Partial energy level diagram of Sm^{3+}- ions in KNbSiSm10 glass showing excitation, radiative, non- radiative decays and possible cross-relaxation channels.

Table4. The experimental lifetime (τ_{exp}, ms), of $^4G_{5/2}$ level, energy transfer parameters (Q), critical transfer distances (R_0, Å) and donor-acceptor interaction parameters (C_{DA}, X 10^{-41} cm^6/s), for different Sm^{3+} - concentrations in KNbSiSm glasses

Glass	τ_{exp}	Q	R_0	C_{DA}
KNbSiSm0.05	1.19	---	---	---
KNbSiSm0.1	1.22	---	---	---
KNbSiSm0.5	0.93	0.54	12.44	194
KNbSiSm1.0	0.71	0.95	9.54	39
KNbSiSm2.0	0.42	2.02	8.37	18

4. Conclusions

Potassium niobate silicate glasses with different concentrations of Sm^{3+}- ions were prepared and characterized for their structural and optical properties through Raman, absorption, excitation, emission and decay measurements at room temperature. The Raman spectrum revealed the basic structural units related to the presence of Si- O- Si and Nb- O bands which are attributed to NbO_6 octahedral with non-bridging oxygen's. Judd- Ofelt(JO) parameters Ω_λ (λ=2, 4, 6) have been evaluated from the oscillator strengths of absorption bands in UV- Vis/NIR regions. Various radiative parameters like radiative transition probabilities(A_R, s^{-1}), peak stimulated emission cross- sections $\sigma_e(\lambda_p)$, experimental (β_{exp}) and calculated (β_R) branching ratios for the emission transitions of Sm^{3+} ion in KNbSiSm10 glass. From these results it is suggested that Sm^{3+}-doped potassium niobate silicate glasses are more efficient luminescent materials for the development of lasers and photonic devices in the visible region.

Acknowledgements

One of the authors CKJ is grateful to MoU-DAE-BRNS, Govt. of India for the sanction of major research project (No.2009/34/36/BRNS/3174, dt.12-02-2010) under MoU between S.V.University, Tirupati and BARC, Mumbai.

Volume : 3 | Issue : 5 | May 2013 | ISSN - 2249-555X

REFERENCE

[1] M. Takahashi, M. Shojiya, R. Kawamoto, K. Kadono, T. Ohtuki, and N. Peyghambarian, J. Appl. Phys., vol. 81, pp. 2940, 1997. | [2] S. Q. Xu, Z. M. Yang, J. J. Zhang, G. N. Wang, S. X. Dai, L. L. hu, and Z. H. Jiang, Chem. Phys. Lett., vol. 385, pp. 263, (2004). | [3] N. L. Dai, L. Hu, J. Yang, S. Dai, and A. Lin, J. Alloys. Compd., vol. 363, pp. 1, 2004. | [4] J. H. Campbell, and T. I. Suratwala, J. Non-Cryst. Solids, vol. 263&264,pp. 318, 2000. | [5] M. Zambelli, M. Abril, V. Lavin, A. Speghini, and M. Bettinelli, J. Non-Cryst. Solids, vol. 345&346, pp. 386, 2004. | [6] V. Venkatramu, P. Babu, C. K. Jayasankar, Th. Troster, W. Sievers, G. Wortmann, Opt. Mater., vol.29, pp. 1429, 2007. | [7] B. R. Judd, Phys. Rev., vol. 127, pp. 750, 1962. | [8] G. S. Ofelt, J. Chem. phys., vol. 37, pp. 511, 1962. | [9] J. S. Wang , E. M. Vogel, E. Suitzer, Opt. Mater., vol. 3, pp.187,1994. | [10] W. L. Konijnendijk. Glastechn. Ber., vol. 48, pp. 216, 1975. | [11] Y. Tsunawaki, N. Iwamoto, T. Hattori, A. Mitsuishi, J. Non-Cryst. Solids ,vol. 44, pp. 369, 1981. | [12] Z. Wang, B. Sui, S. Wang, H. Liu, J. Non- Cryst. Solids,vol. 80: pp. 60,1986. | [13] G. E. Rachkovkaya, N. M.Bobkova, J. Non-Cryst. Solids ,vol. 90, pp. 617, 1987. | [14] K. Fukumi, S. Sakka, J. Mater. Sci. Letters, vol. 23, pp. 2819, 1988. | [15] A. Shtin and V. Mamochin, Fiz. Khim. Stekla , vol. 8: pp. 170,1982. | [16] V. Kolobkov, E. Kolobkova, I. Mararov and V. Mamoshin, Fiz. Khim. Stekla, vol.1: pp. 352, 1986. | [17] R. Praveena, V. Venkatramu, P. Babu, and C. K. Jayasankar, PhysicaB, vol.403, pp.3527, 2008. | [18] W. T. Carnall, P. R. Fields, K.Rajnak, J. Chem. Phy., vol. 49, pp. 4424, 968. | [19] C. K. Jayasankar, P. Babu, J. Alloys. Compds., vol. 307, pp. 82, 2000. | [20] A. Kumar, D. K. Rai, and S. B. Rai, Spectro Chim Acta A Part A, vol.59, pp. 917, 2003. | [21] G. Ingletto, M. Bettinelli, L. D. Sipio, F. Negrisolo, C. Aschieri, Inorg. Chim. Acta, vol. 188, pp. 201, 1991. | [22] B. C. Jamalaiah, J. Suresh Kumar, A. Mohan Babu, T. Suhasini and L. Rama Moorthy, J. Lumin., vol. 129, pp. 363, 2009. | [23] P. Nachimuthu, R. Jagannathan, V. Nirmal Kumar, D. Narayana Rao, J. Non- Cryst. Solids, vol. 217, pp. 215, 1997. | [24] I. Arul Rayappan, K. Selvaraju and K. Marimuthu, Physica B, vol. 406, pp.548, 2011. | [25] P. Srivastava, S. B. Rai and D. K. Rai, Spectrochim. Acta A, vol. 60: pp. 637, 2004. | [26] Ch. Srinivasa Rao, C. K. Jayasankar, Optics Comm., vol. 286, pp. 204. 2013. | [27] G. H. Dieke, Spectra and energy levels of rare earth ions in crystals, Wiely, Newyork, 1968. | [28] M. Inokuti, F. Hirayama, The Journal of Chem. Phy., vol. 43, pp. 978, 1965. |